

Published in final edited form as:

*Cancer Lett.* 2014 October 10; 353(1): 59–67. doi:10.1016/j.canlet.2014.07.002.

## Antiproliferative activity of novel imidazopyridine derivatives on castration-resistant human prostate cancer cells

Sakthivel Muniyan<sup>a</sup>, Yu-Wei Chou<sup>a,b</sup>, Matthew A. Ingersoll<sup>a</sup>, Alexis Devine<sup>c</sup>, Marisha Morris<sup>d</sup>, Valerie A. Odero-Marah<sup>d,e</sup>, Shafiq A. Khan<sup>d,e</sup>, William G. Chaney<sup>a</sup>, Xiu R. Bu<sup>c,f</sup>, and Ming-Fong Lin<sup>a,g,h,i,\*</sup>

<sup>a</sup>Department of Biochemistry and Molecular Biology, University of Nebraska Medical Center, Omaha, NE, USA

<sup>b</sup>Kaohsiung Chang Gung Memorial Hospital, Kaohsiung, Taiwan, ROC

<sup>c</sup>Department of Chemistry, Clark Atlanta University, Atlanta, GA, USA

<sup>d</sup>Department of Biological Sciences, Clark Atlanta University, Atlanta, GA, USA

<sup>e</sup>Center for Cancer Research and Therapeutic Development, Clark Atlanta University, Atlanta, GA, USA

<sup>f</sup>Laboratory for Electro-Optical Materials & NASA Center for High Performance Polymers and Composites, Clark Atlanta University, Atlanta, GA, USA

<sup>g</sup>Eppley Institute for Research in Cancer and Allied Diseases, University of Nebraska Medical Center, Omaha, NE, USA

<sup>h</sup>Department of Surgery/Urology, University of Nebraska Medical Center, Omaha, NE, USA

<sup>i</sup>College of Pharmacy, Kaohsiung Medical University, Kaohsiung, Taiwan 807, ROC

### Abstract

Metastatic prostate cancer (mPCa) relapses after a short period of androgen deprivation therapy and becomes the castration-resistant prostate cancer (CR PCa); to which the treatment is limited. Hence, it is imperative to identify novel therapeutic agents towards this patient population. In the present study, antiproliferative activities of novel imidazopyridines were compared. Among three derivatives, PHE, AMD and AMN, examined, AMD showed the highest inhibitory activity on LNCaP C-81 cell proliferation, following dose- and time-dependent manner. Additionally, AMD exhibited significant antiproliferative effect against a panel of PCa cells, but not normal prostate epithelial cells. Further, when compared to AMD, its derivative DME showed higher inhibitory

© 2014 Elsevier Ireland Ltd. All rights reserved

\*Corresponding Author: Ming-Fong Lin, Ph. D. Department of Biochemistry and Molecular Biology College of Medicine University of Nebraska Medical Center 985870 Nebraska Medical Center Omaha, NE 68198-5870, USA TEL: (402) 559-6658 FAX: (402) 559-6650 mlin@unmc.edu.

**Publisher's Disclaimer:** This is a PDF file of an unedited manuscript that has been accepted for publication. As a service to our customers we are providing this early version of the manuscript. The manuscript will undergo copyediting, typesetting, and review of the resulting proof before it is published in its final citable form. Please note that during the production process errors may be discovered which could affect the content, and all legal disclaimers that apply to the journal pertain.

### Conflict of interest statement

We do not have any conflict of interest

activities on PCa cell proliferation, clonogenic potential and *in vitro* tumorigenicity. The inhibitory activity was apparently in part due to the induction of apoptosis. Mechanistic studies indicate that AMD and DME treatments inhibited both AR and PI3K/Akt signaling. The results suggest that better understanding of inhibitory mechanisms of AMD and DME could help design novel therapeutic agents for improving the treatment of CR PCa.

## 1. Introduction

Prostate cancer (PCa) is the second leading cause of cancer deaths in United States men [1]. Androgen-deprivation therapy (ADT) has been the mainstay of treatment towards patients with metastatic PCa [2,3]. Although most of PCa respond well to ADT initially, most PCa relapse and become the castration-resistant (CR) PCa [2,3]. CR PCa is lethal with about 18-month median survival time [4]. Currently, chemotherapy is the standard-of-care treatment for CR PCa. Nevertheless, it only provides a minimal improvement in survival. Hence, the prime need is to identify a novel therapeutic agent to improve the efficacy of CR PCa treatment.

Imidazopyridine derivatives are a class of novel compounds which have aromatic aldehydes and a pyridine group, and possess medicinal importance [5-7]. Recent studies show imidazopyridine derivatives exhibit potent antitumor activity against breast and pancreatic cancers [8,9]. Nevertheless, no report is currently available on the antiproliferative effect of imidazopyridine derivatives on CR PCa. Therefore, the present study is undertaken to synthesize a series of novel imidazopyridine derivatives and to investigate their antiproliferative effect against a panel of PCa cancer cell lines including both AR-positive and AR-negative AI PCa cells which exhibit diverse phenotypes of CR PCa. Our results show that imidazopyridine derivatives inhibit CR PCa cell proliferation, decrease migration and *in vitro* tumorigenicity. Our data, to the best of our knowledge, is the first report that clearly shows the potential of this family of compounds to serve as effective molecules towards CR PCa treatment by inhibiting AR and PI3K/Akt signaling.

## 2. Materials and methods

### 2.1. Materials

RPMI 1640, Keratinocyte SFM medium, gentamicin, and L-glutamine were from Invitrogen (Carlsbad, CA, USA). Fetal bovine serum (FBS) and charcoal/dextran-treated FBS were purchased from Atlanta Biologicals (Lawrenceville, GA, USA). Polyclonal antibodies (Abs) recognizing all three isoforms of Shc protein were obtained from Upstate (Lake Placid, NY, USA). Anti-cyclin B1, anti-cyclin D1, anti-AR, anti-Bax, anti-Bcl<sub>XL</sub>, anti-PCNA, anti-p53, anti-PSA and horseradish peroxidase-conjugated anti-mouse, anti-rabbit, anti-goat IgG Abs and Akt inhibitor (MK2206) were all from Santa Cruz Biotechnology (Santa Cruz, CA, USA). Anti-phospho-Akt(Ser473) and anti-Akt Abs were from Cell Signaling Technology (Beverly, MA, USA). Anti- $\beta$ -actin Ab and DHT were obtained from Sigma (St. Louis, MO, USA). PI3K inhibitor (LY294002) was obtained from Calbiochem (San Diego, CA, USA).

## 2.2. Synthesis of Imidazopyridines

The synthesis of the imidazopyridine compounds were essentially followed the protocol described in our previous publication [7]. All the reactions were performed in flame-dried glassware under the nitrogen environment using freshly diluted solvents. All the chemicals and solvents were used as received. <sup>1</sup>H NMR (400 MHz) and <sup>13</sup>C NMR (100 MHz) spectra were recorded with TMS as an internal standard for reference. The C, H, and N contents were obtained through combustion analysis. Melting points are uncorrected. The compounds were synthesized using a mixture consisting of di-2-pyridyl ketone, substituted aromatic aldehydes and ammonium acetate in 35 mL of glacial acetic acid [7]. Briefly, phenol, 4-actetamido-benzaldehyde, benzenamine and N-N-dimethyl aniline were used as substituted aldehydes to synthesize IMP-PHE, -AMN, -AMD and -DME, respectively (Fig. 1). The reaction was stirred at 110°C under N<sub>2</sub> and was monitored by TLC (EtOAc:Hex=1:1) alumina plates. Upon completion, the reaction was allowed to cool to room temperature and poured into 200 mL of ice water. The yielded solid was filtered, dried, and recrystallized with appropriate solvent to obtain an analytically pure compound [7].

## 2.3. Cell culture

Human prostate carcinoma cell lines LNCaP, MDA PCa2b, PC-3, DU 145 and immortalized normal prostate epithelial cells RWPE1 and PZHPV-7 cells were all obtained from the American Type Culture Collection (Rockville, MD, USA) and maintained as described [10-11]. LNCaP, PC-3 and DU 145 cells were routinely maintained in the regular culture medium, i.e., phenol red-positive RPMI 1640 medium supplemented with 5% FBS, 2 mM glutamine and 50 µg/mL gentamicin. LNCaP C-81 cells were described previously [12,13], and exhibit the CR phenotype including functional AR expression and prostate-specific antigen (PSA) secretion with rapid cell growth in the steroid-deprived condition [12-13]. Further, those cells exhibit the intracrine regulatory mechanism [14]. Similarly, MDA PCa2b-AI cells exhibit androgen-independent (AI) proliferation and were obtained as described [10,15,16]. MDA PCa2b-AI cells were cultured in BRFF-HPC1 medium containing 20% FBS, 2 mM glutamine and 50 µg/mL gentamicin [10,16]. RWPE1 and PZHPV-7 cells were grown in Keratinocyte-SFM supplemented with bovine pituitary extract (25 µg/mL) and recombinant epidermal growth factor (0.15 ng/mL) containing 50 µg/mL gentamicin.

For steroid-starvation, cells were maintained in steroid-reduced (SR) media, i.e., phenol red-free RPMI 1640 medium containing 5% heat-inactivated, charcoal/dextran-treated FBS (v/v), 2 mM glutamine, 50 µg/mL gentamicin and 1 nM 5α-dihydrotestosterone (DHT), which mimics the condition of androgen ablation treatment in patients. PHE, AMN, AMD and DME were dissolved in DMSO as 1,000× concentrated stock solutions, stored at -20°C, and diluted in the respective culture media at the time of use. Control cells were treated with media containing an equal amount of DMSO.

## 2.4. Cell proliferation assay

For the cell proliferation assay in regular media, LNCaP C-81 cells were plated at a density of  $2 \times 10^3$  cells/well in 6-well plates for 3 days and then treated with 10 µM of PHE, AMN or AMD in fresh media for 3 days. To compare the effect of AMD on different prostate cells,

PCa cells and immortalized normal prostate epithelia were plated in their respective regular media at the described cell density for 3 days, followed by the addition of 10  $\mu$ M AMD in fresh media. The cell numbers were counted using a Cellometer Auto T4 Image-based cell counter (Nexcelom Bioscience), which cell number was counted by Trypan blue exclusion assay. The ratio of live cell number in the experimental group to that of the control group was calculated for indicating cell proliferation.

To determine the effect of AMD and DME in SR media, C-81 cells were plated in regular medium for 3 days and then steroid-starved for 2 days in a SR medium. After being fed with fresh SR medium, cells were treated with different concentrations of AMD or DME. Control cells were treated with solvent alone. The cell numbers were counted and the ratio of cell growth was calculated as described above.

## 2.5. Kinetics of cell growth determination

To determine the time-dependent effect of AMD and DME on the growth of LNCaP C-81 cells, cells were seeded on six-well culture plates with triplicates and maintained in regular culture medium for three days. For SR condition, cells were maintained for additional 48 hours in SR medium. One set of attached cells from each culture condition was harvested and counted as day 0 as described above. The remaining attached cells were fed with fresh regular or SR medium containing solvent, AMD or DME, and harvested on days 1, 3 and 5 for total cell number counting. The fresh medium was added to the remaining LNCaP cells on days 1 and 3.

## 2.6. Immunoblot analysis

To analyze cellular proteins, cells were harvested by scraping. The cell pellet was rinsed with ice-cold 20 mM HEPES-buffered saline (pH 7.0), lysed in ice-cold cell lysis buffer containing protease and phosphatase inhibitors, and the total lysate protein was prepared accordingly [12,17]. An aliquot of total cellular lysate proteins was electrophoresed on SDS–polyacrylamide gels (7.5–12% acrylamide) for western blot analyses [12]. The proteins of interest were visualized by an ECL detection system.  $\beta$ -actin was detected as a loading control.

## 2.7. Cell migration

Cell migration was determined using an *in vitro* ‘wound-healing’ assay. Briefly, PC-3 cells were seeded in 6-well plates and grown for 48 hours to reach confluence. Wounds were made in the confluent cell monolayer using a sterilized P200 pipette tip. The wound was washed with RPMI medium without FBS to remove all the detached cell debris. Remaining cells were treated with fresh media, media containing 10  $\mu$ M AMD or DME. After 12 hours, cells were stained with crystal violet and images were taken. The wound gap was measured, and % wound healing was calculated. The average % of wound healing was determined by at least 3 measurements per scratch from 2 independent experiments.

## 2.8. Clonogenic cell growth assay and Anchorage-independent soft agar assay

The clonogenic cell growth was described previously [15,18]. Briefly, LNCaP C-81 cells were plated in regular culture medium at densities of 20, 200, and 2,000 cells per well in 6-

well plates. After overnight incubation, unattached cells were removed and attached cells were fed with fresh regular medium with or without respective compounds. Two milliliters of fresh medium containing respective compound were added into each well on Days 5 and 8. On Day 10, the attached cells were stained with 0.2% crystal violet solution containing 50% methanol.

The anchorage-independent growth of cells was determined by soft agar analysis with modifications [18]. Briefly,  $5 \times 10^4$  cells were seeded in 0.25% agarose on the top of a base layer containing 0.3% agarose. One day after seeding, cell clumps containing more than one cell were excluded from the study, and the cells were fed with fresh medium containing respective treatment compounds once in every three days. The colony number was counted after 4 weeks of incubation at 37°C. Alternatively, the colonies were stained with 0.1% crystal violet solution containing 20% methanol and counted.

## 2.9. Statistical analysis

Each set of experiments was performed in duplicate or triplicate, as specified in the figure legend or experimental design, repeated at least two or three times as independent experiments. The mean and standard error values of experimental results were calculated. A Student-t test was used for comparison between each group.  $p < 0.05$  was considered statistically significant [18]. The relationship between the relative ratios of cell proliferation and the dosage of compounds was evaluated by their correlation coefficient ( $r$ ). The correlation was considered significant when the  $p$ -value was less than 0.05.

## 3. Results

### 3.1. Anti-proliferative effect of imidazopyridine derivatives on LNCaP C-81 PCa cells

To determine the anti-proliferative effect of imidazopyridine derivatives, a cell proliferation assay was initially performed in LNCaP C-81 PCa cells because these cells exhibit many biochemical properties of the advanced CR PCa phenotype [12-14]. After 72 hour treatment with 10  $\mu$ M imidazopyridine derivatives in the regular cell culture medium, all three compounds PHE, AMD and AMN reduced cell proliferation by an average of 42%, 53% and 18%, respectively (Fig. 2A). The antiproliferative activity of these compounds respectively correlated with decreased protein levels of proliferation markers cyclin B1, cyclin D1 and PCNA in those cells (Fig. 2B). In AMD-treated LNCaP C-81 cells, AR protein level was also decreased and tumor suppressor p53 and proapoptotic protein Bax were elevated (Fig. 2B). Since AMD exhibited the highest inhibitory activity among the three compounds examined, AMD compound was used for further experiments.

### 3.2. Dose- and time-dependent effects of AMD on LNCaP C-81 cells

We examined the dose-dependent effect of AMD on LNCaP C-81 cells. Upon treated with 0-10  $\mu$ M AMD for 72 hours, cell growth was analyzed. In regular culture media, AMD inhibited LNCaP C-81 cell growth in a dose-dependent manner (Fig. 2C). 10  $\mu$ M AMD inhibited 54% cell growth and were used in future experiments.

To determine the kinetic effect of AMD, at each time point, cells in triplicates from each group were harvested and cell number determined. The remaining cells were fed with fresh media or media plus AMD. As shown in Fig. 2D, after 24-hour treatment, cell growth was decreased by about 19%. Upon 72-hour treatment, approximately 53% growth inhibition was observed. Five-day treatment with 10  $\mu$ M AMD inhibited the cell growth by over 60% (Fig. 2D). Thus, AMD suppressed LNCaP C-81 cell growth following a time course.

### 3.3. Antiproliferative effect of AMD on AR-positive and AR-negative PCa cells in comparison with immortalized normal prostate epithelial cells

The growth suppressive efficacy of 10  $\mu$ M AMD was evaluated in a panel of AI cells including both AR-positive (LNCaP C-81 and MDA PCa2b AI) and AR-negative (PC-3 and DU145) PCa cells. Significant growth inhibition on all PCa cells tested was observed at 10  $\mu$ M AMD (Fig. 2E). Notably, 10  $\mu$ M AMD had only approximately 10% effect on the proliferation of immortalized normal prostate epithelial RWPE1 and PZHPV-7 cells (Fig. 2E). Together, our results showed that AMD exhibits potent inhibitory activity on AI PCa cell growth, but not normal prostate epithelia.

### 3.4. Comparative effects of AMD and DME in LNCaP C-81 cells

To improve the efficacy of AMD on inhibiting AI PCa cell growth, the amino functional group of AMD was modified and a new derivative DME was obtained (Fig. 1). Preliminary experiments revealed that 10  $\mu$ M DME of 72 hour-treatment decreased LNCaP C-81 cell proliferation by up to 88% ( $p < 0.001$  vs control, data not shown); while AMD inhibited cell growth by about 55% (data not shown and Fig. 2A). We then examined the dose-dependent effect of DME on LNCaP C-81 cells for 72 hours. Our results showed both AMD and DME inhibit cell growth in a dose-dependent manner (Fig. 3A vs. Fig. 2C). In regular culture media, the efficacy of growth inhibition by DME was about two fold that of AMD (Fig. 3) with IC<sub>50</sub> value of about 3.9  $\mu$ M and 7.5  $\mu$ M, respectively.

We analyzed the effect of AMD and DME in a SR medium containing 1 nM DHT, which mimics the clinical condition under androgen deprivation treatment. The same trend of dose-dependent inhibition was observed despite the inhibitory activity was decreased (Fig. 3B). In SR conditions, DME inhibited cell growth with IC<sub>50</sub> of 6.3  $\mu$ M, comparing with 11.4  $\mu$ M of AMD. We thus performed further studies on AMD and DME at 10  $\mu$ M in SR condition for clinical relevance.

### 3.5. Effects of AMD and DME on cell migration and in vitro tumorigenicity

The effects of AMD and DME on PCa cell migration were assessed by a wound healing assay with PC-3 cells as the model system since C-81 cells exhibit slow-migration (data not shown). As shown in Fig. 4A, both AMD and DME significantly inhibited PC-3 cell migration. After 12 hours, 50-60% of the wound area remained open in AMD- and DME-treated cells, while the wound in solvent-treated control group was completely closed ( $p < 0.01$  with control).

To explore the anti-tumorigenic potential of AMD and DME, a clonogenic assay was performed on LNCaP C-81 cells. As shown in Fig. 4B, after 10 day- treatment, both AMD



and DME inhibited clonogenic growth. In comparison, DME inhibited clonogenic growth at all cell densities examined, while AMD had less inhibitory activity with colonies clearly seen in 2000 cells/well. Nevertheless, the size of AMD-treated colony was dramatically reduced, much smaller than controls.

An *in vitro* anchorage-independent soft agar assay was performed on LNCaP C-81 cells. As shown in Figs. 4C and 4D, after 4-week cultured at a density of 5000 cells per 35 mm dish there was visible colony formation in solvent-treated control groups. AMD treatment decreased the soft agar colony number by about 50%, and DME treatment inhibited over 90% (Fig. 4D). Further, both AMD and DME greatly reduced the size of colonies. Therefore, both AMD and DME exhibit anti-tumorigenic effects on both AI PC-3 and LNCaP C-81 cells (Fig. 4).

### 3.6. Kinetics of AMD and DME effects on LNCaP C-81 cell proliferation in SR condition

We investigated the kinetics of AMD and DME on LNCaP C-81 cell proliferation in SR conditions. As shown in Fig. 5A, after 3-day treatment in SR conditions, both AMD and DME significantly inhibited the growth of LNCaP C-81 cells, and DME exhibited a better efficacy than AMD. It should be noted that in SR conditions, while control cells continuously grew on day 3 and 5, the cell number of AMD- and DME-treatment declined. Upon 5-day DME-treatment, the cell number was even lower than the pre-treatment day 0 cell number. The decrease in cell growth was reflected by cyclin D1 protein level (Fig. 5B).

### 3.7. Effects of AMD and DME on AR and Shc level in SR conditions

Since the majority of CR PCa cells still express functional AR for their growth requirement [19], we analyzed AR protein level in AMD- and DME-treated LNCaP C-81 cells under SR condition. Fig. 5B showed AR protein level was greatly reduced in both AMD- and DME-treated cells at day 3 and day 5 after an initial elevation in day one. Concurrently, the cellular level of PSA, an androgen-regulated protein, was closely associated with AR protein level. Thus, AMD- and DME-treatments decrease AR signaling.

The protein level of p66Shc, a 66 kDa Src homologous-collagen homologue (Shc), is involved in regulating the proliferation of several carcinoma cells including PCa cells and can be up-regulated by steroids [20-23]. Fig. 5B showed the protein level of p66Shc but not p52Shc or p46Shc was decreased in 3-day and 5-day AMD- and DME-treated cells. The decreased p66Shc protein level correlates with diminished cell proliferation, AR and cyclin D1 protein levels.

### 3.8. Apoptotic effects of AMD and DME

We investigated whether AMD and DME suppress cell growth in part by inducing cell apoptosis since the 5-day DME-treated cell number was lower than the day 0 control. Bcl-X<sub>L</sub>, an anti-apoptotic factor [24], and Bax, a proapoptotic protein [25], were analyzed in AMD- and DME-treated cells. Treatment of LNCaP C-81 cells with AMD and DME caused time-dependent upregulation of Bax protein seen at day 3 and day 5 (Fig. 5C). At day 5, p53 protein, a tumor suppressor, was also elevated in both AMD- and DME-treated cells (Fig. 5C). In parallel, AMD and DME treatments caused a significant decrease of Bcl-X<sub>L</sub> protein,

compared to untreated control cells (Fig. 5C). These results together indicate that induction of apoptosis is one mechanism by which imidazopyridine derivatives induce growth suppression in PCa cells under steroid-reduced conditions.

### 3.9. Effect of AMD and DME on AR and PI3K/Akt signaling

Akt activation due to loss of PTEN activity can potentially support CR PCa formation [26-28]. In parallel, aberrant AR signaling plays a critical role in CR PCa progression [19,29,30]. Hence, it is proposed that the combined inhibition of AR and PI3K/Akt can effectively improve the therapeutic efficacy in CR PCa patients. We determined whether AMD and DME can inhibit PI3K/Akt by examining S473 phosphorylation of Akt in LNCaP C-81 cells in which Akt is fully activated by S473 phosphorylation [16]. We used PI3K and Akt inhibitors for comparison. Fig. 6 showed that AMD and DME treatments decreased the S473-phosphorylation of Akt in addition to decreased AR and PSA proteins in LNCaP C-81 cells (Figs. 5B and 6). As expected, both PI3K and Akt inhibitors respectively reduced Akt(S473) phosphorylation (Fig. 6). Interestingly, Akt inhibition greatly increased cellular prostatic acid phosphatase (cPAP) level, a tumor suppressor gene in PCa [31], but not PI3K inhibition (Fig. 6). Unexpectedly, AR protein level was respectively elevated following PI3K and Akt inhibitor treatments (Fig. 6). The elevated AR expression level was corroborated by the increased cellular PSA level.

## 4. Discussion

In androgen-dependent cells, upon androgen binding, AR is activated and then translocated to nucleus for gene regulation, resulting in cell growth and survival [29,30,32]. Nevertheless, CR PCa cells, which still require functional AR, evade ligand-dependent and ligand-independent mechanisms that allow cells to survive in an androgen-depleted environment [14,29,30,32-34]. Thus, targeting multi-functional molecules simultaneously can improve the efficacy of therapy.

In the present study, LNCaP C-81 cells were used as the primary cell model for our studies because these cells exhibit many properties of CR PCa [12-14,33]. We first demonstrated the antiproliferative efficacy of three novel imidazopyridine derivatives on LNCaP C-81 cells (Fig. 2). Among them, AMD effectively inhibits the cell growth evidenced by decreased cell number and cyclin protein levels (Fig. 2). Further, Bax and p53, a Bax transcription factor [34], are upregulated in AMD-treated cells. Hence, AMD inhibits cell proliferation. Importantly, while AMD has a broad spectrum of antiproliferative activity in both AR-positive and AR-negative AI PCa cells; AMD spares normal prostate epithelial cells (Fig. 2E).

To improve the efficacy of growth suppression on AI PCa cells, we modified the amino group side chain of AMD and obtained a derivative termed DME (Fig. 1). DME exhibits superior inhibitory activity compared to AMD on LNCaP C-81 cell growth in regular as well as SR media (Fig. 3). While both AMD and DME effectively inhibit LNCaP C-81 and PC-3 cell proliferation (Figs. 3&5), these two compounds may exhibit different mechanisms of inhibition towards these two cell lines. For example, in the wound healing assay, AMD was a more potent inhibitor of PC-3 cell migration than DME. Unfortunately, LNCaP C-81



cells migrate too slowly to conduct a wound healing assay. Conversely, in both clonogenic and soft agar assays conducted on LNCaP C-81 cells, DME was a more potent inhibitor of colony formation than AMD (Fig. 4). One possible explanation of differential effects by DME vs. AMD is that DME is more potent than AMD at inhibiting AR protein level and Akt activation in C-81 cells. Additionally, PC-3 cells are AR-negative and LNCaP C-81 cells express functional AR; as such, DME and AMD inhibit both AR and Akt in LNCaP C-81 cells, while only inhibit Akt in PC-3 cells. Together, DME is more potent than AMD at inhibiting LNCaP C-81 cell proliferation and colony formation. Nevertheless, further experiments with direct comparison are required to delineate the mechanism of growth suppression by DME vs. AMD on these two cell lines.

Targeting AR and/or intervening with androgen biosynthesis can effectively inhibit CR PCa and thus improve patient survival [35-38]. Our results show for the first time that both AMD and DME treatments can decrease AR protein and signaling with cell growth suppression (Figs. 2, 5A and 5B). Although the mechanism of AR inhibition by imidazopyridine derivatives requires further investigation, our results show that imidazopyridine derivatives inhibit AR-positive PCa cell growth in part by inhibiting AR signaling, evidenced by decreased PSA protein (Figs. 5B and 6). It is possible that imidazopyridine derivatives decrease AR protein partly by inhibiting Akt phosphorylation. AMD and DME inhibit Akt-induced AR protein stability, contributing to observed lower levels of AR protein. Furthermore, by inhibiting AR signaling, AMD and DME may prevent the interaction of AR with p85 $\alpha$  regulatory subunit of PI3K; which results in decreased Akt activation [39]. p66Shc, a 66 kDa oxidase, can up-regulate cell growth and is elevated in steroid-regulated carcinomas [20,23,40]. In PCa, p66Shc plays a role in mediating the cross-talk signal between steroids and tyrosine phosphorylation [40], which is involved in regulating cell proliferation and apoptosis [22,23,40,41]. Further, androgens upon binding to AR can up-regulate p66Shc protein level and PCa cell proliferation [40]. Our data show that both AMD- and DME-treatments resulted in decreased AR and p66Shc protein levels, correlating with diminished cell proliferation and elevated apoptotic Bax protein (Fig. 5). Although LNCaP C-81 PCa cells are androgen-independent cells, their growth is still increased upon androgen treatment [13,14,19]. Thus, imidazopyridine derivatives inhibition of AR-mediated cell growth and p66Shc protein levels is at least in part through decreased AR protein levels. Thus, p66Shc protein may serve as a common convergent point that integrates cell proliferation and apoptosis signaling [23].

CR PCa cells often have elevated levels of anti-apoptotic molecules for its survival [29,42]. Bcl-2 family members play critical roles in regulating apoptosis. For example, Bcl-X<sub>L</sub> is anti-apoptosis [43,44] and can also enhance metastasis [45]; while Bax can heterodimerize with Bcl-X<sub>L</sub> and its increased level favors apoptosis [25,46]. Further, p53 protein is a tumor suppressor, a Bax transcriptional regulator [34,47] and also mediates a Bcl-2 family member-independent apoptosis process. The elevated Bax and p53 with decreased Bcl-X<sub>L</sub> proteins (Fig 5C) together indicate AMD and DME can induce apoptosis. Therefore, we observed DME- and AMD-induced growth suppression and DME-treated cells had cell number even lower than that of day 0 control cells (Fig. 5A).

The PI3K/Akt signaling pathway plays a vital role in cell growth and survival; its dysregulation contributes to therapeutic resistance of tumor cells [26,27,29,30,48]. Our results show AMD and DME inhibit Akt activation in addition to AR signaling (Figs. 5 and 6). Unexpectedly, treatments with both PI3K and Akt inhibitors induce AR and PSA levels in PTEN-inactive LNCaP C-81 cells (Fig. 6), which is consistent with the observation on the reciprocal activation of AR and PI3K signaling in PTEN-deficient mouse PCa cells [28]. Hence, the data indicate that patients treated with PI3K pathway inhibitors can experience a rise in PSA levels if their tumors are PTEN deficient [28]. Further, it is also hypothesized that Akt activation may inhibit HER-2-mediated AR activation [28]. Our results clearly show that these novel imidazopyridine derivatives significantly inhibit both AR and PI3K/Akt signaling. Even though targeting either AR or PI3K/AKT signaling alone by second generation inhibitors has shown promising results [28,49]; the activation of reciprocal pathways can counteract the efficacy of inhibitors targeting single signaling pathway in PCa [28,50]. Hence, combination therapy targeting both AR and PI3K/Akt signaling molecules would improve the therapeutic efficacy toward CR PCa.

In summary, our data show for the first time that imidazopyridine derivatives can effectively inhibit CR PCa cell proliferation in SR conditions and reduce in vitro tumorigenicity. The concurrent inhibition of PI3K/Akt and AR signaling with the activation of apoptotic pathway is one of the underlying mechanisms that imidazopyridine derivatives suppress CR PCa cell growth. Our data thus support the notion that the imidazopyridine derivatives represent a promising class of compounds to combat CR PCa. Further studies are needed to elucidate the underlying suppression mechanisms on CR PCa cells. Modifications of other functional groups of these compounds may further improve the efficacy of PCa suppression for treating CR PCa.

## Acknowledgments

This work was supported in part by the National Cancer Institute, National Institutes of Health [R01 CA88184]; Department of Defense PCa Training Grant [PC094594, PC121645]; and the University of Nebraska Medical Center Bridge Fund.

## Abbreviations:

<b>ADT</b>	androgen deprivation therapy
<b>AI</b>	androgen-independent
<b>AR</b>	androgen receptor
<b>AS</b>	androgen-sensitive
<b>CR PCa</b>	castration-resistant prostate cancer
<b>DHT</b>	dihydrotestosterone
<b>ECL</b>	enhanced chemiluminescence
<b>FBS</b>	fetal bovine serum
<b>PCa</b>	prostate cancer

<b>PI3K</b>	phosphatidylinositol-3 kinase
<b>PSA</b>	prostate-specific antigen
<b>p66Shc</b>	a 66 kDa Src homologous-collagen homologue
<b>SR</b>	steroid-reduced

## References

- [1]. Siegel R, Naishadham D, Jemal A. Cancer statistics. *C.A. Cancer J. Clin.* 2013; 62:10–29.
- [2]. Smalet O, Scher HI, Small EJ, Verbel DA, McMillan A, Regan K, Kelly WK, Kattan M. Nomogram for overall survival of patients with progressive metastatic prostate cancer after castration. *J. Clin. Oncol.* 2002; 20:3972–3982. [PubMed: 12351594]
- [3]. Asmane I, Céraline J, Duclos B, Rob L, Litique V, Barthélémy P, Bergerat JP, Dufour P, Kurtz JE. New strategies for medical management of castration-resistant prostate cancer. *Oncology.* 2011; 80:1–11. [PubMed: 21577012]
- [4]. Saad F, Hotte SJ. Guidelines for the management of castrate-resistant prostate cancer. *Can. Urol. Assoc. J.* 2010; 4:380–384. [PubMed: 21191494]
- [5]. Terao Y, Suzuki H, Yoshikawa M, Yashiro H, Takekawa S, Fujitani Y, Okada K, Inoue Y, Yamamoto Y, Nakagawa H, Yao S, Kawamoto T, Uchikawa O. Design and biological evaluation of imidazo[1,2-a]pyridines as novel and potent ASK1 inhibitors. *Bioorg. Med. Chem. Lett.* 2012; 22:7326–7329. [PubMed: 23147077]
- [6]. Newhouse BJ, Wenglowsky S, Grina J, Laird ER, Voegtli WC, Ren L, Ahrendt K, Buckmelter A, Gloor SL, Klopfenstein N, Rudolph J, Wen Z, Li X, Feng B. Imidazo[4,5-b]pyridine inhibitors of B-Raf kinase. *Bioorg. Med. Chem. Lett.* 2013; 23:5896–5899. [PubMed: 24042006]
- [7]. Wang J, Dyers L Jr, Mason R Jr, Amoyaw P, Bu XR. Highly efficient and direct heterocyclization of dipyrindyl ketone to N,N-bidentate ligands. *J. Org. Chem.* 2005; 70:2353–2356. [PubMed: 15760230]
- [8]. Li GY, Jung KH, Lee H, Son MK, Seo J, Hong SW, Jeong Y, Hong S, Hong SS. A novel imidazopyridine derivative, HS-106, induces apoptosis of breast cancer cells and represses angiogenesis by targeting the PI3K/mTOR pathway. *Cancer Lett.* 2013; 329:59–67. [PubMed: 23085493]
- [9]. Yun SM, Jung KH, Lee H, Son MK, Seo JH, Yan HH, Park BH, Hong S, Hong SS. Synergistic anticancer activity of HS-173, a novel PI3K inhibitor in combination with Sorafenib against pancreatic cancer cells. *Cancer Lett.* 2013; 331:250–261. [PubMed: 23340175]
- [10]. Chou YW, Chaturvedi NK, Ouyang S, Lin FF, Kaushik D, Wang J, Kim I, Lin MF. Histone deacetylase inhibitor valproic acid suppresses the growth and increases the androgen responsiveness of prostate cancer cells. *Cancer Lett.* 2011; 311:177–86. [PubMed: 21862211]
- [11]. Chou YW, Zhang L, Muniyan S, Ahmad H, Kumar S, Alam SM, Lin MF. Androgens upregulate Cdc25C protein by inhibiting its proteasomal and lysosomal degradation pathways. *PLoS One.* 2013; 8:e61934. [PubMed: 23637932]
- [12]. Lin MF, Meng TC, Rao PS, Chang C, Schonthal AH, Lin FF. Expression of human prostatic acid phosphatase correlates with androgen-stimulated cell proliferation in prostate cancer cell lines. *J. Biol. Chem.* 1998; 273:5939–5947. [PubMed: 9488733]
- [13]. Igawa T, Lin FF, Lee MS, Karan D, Batra SK, Lin MF. Establishment and characterization of androgen-independent human prostate cancer LNCaP cell model. *Prostate.* 2002; 50:222–235. [PubMed: 11870800]
- [14]. Dillard PR, Lin MF, Khan SA. Androgen-independent prostate cancer cells acquire the complete steroidogenic potential of synthesizing testosterone from cholesterol. *Mol. Cell. Endocrinol.* 2008; 295:115–120. [PubMed: 18782595]

- [15]. Chen SJ, Karan D, Johansson SL, Lin FF, Zeckser J, Singh AP, Batra SK, Lin MF. Prostate-derived factor as a paracrine and autocrine factor for the proliferation of androgen receptor-positive human prostate cancer cells. *Prostate*. 2007; 67:557–571. [PubMed: 17221842]
- [16]. Chuang TD, Chen SJ, Lin FF, Veeramani S, Kumar S, Batra SK, Tu Y, Lin MF. Human prostatic acid phosphatase, an authentic tyrosine phosphatase, dephosphorylates ErbB-2 and regulates prostate cancer cell growth. *J. Biol. Chem.* 2010; 285:23598–23606. [PubMed: 20498373]
- [17]. Meng TC, Lin MF. Tyrosine phosphorylation of c-ErbB-2 is regulated by the cellular form of prostatic acid phosphatase in human prostate cancer cells. *J. Biol. Chem.* 1998; 273:22096–22104. [PubMed: 9705354]
- [18]. Lin MF, Lee MS, Zhou XW, Andressen JC, Meng TC, Johansson SL, West WW, Taylor RJ, Anderson JR, Lin FF. Decreased expression of cellular prostatic acid phosphatase increases tumorigenicity of human prostate cancer cells. *J. Urol.* 2001; 166:1943–1950. [PubMed: 11586265]
- [19]. Scher HI, Sawyers CL. Biology of progressive, castration-resistant prostate cancer: directed therapies targeting the androgen-receptor signaling axis. *J. Clin. Oncol.* 2005; 23:8253–8261. [PubMed: 16278481]
- [20]. Lee MS, Igawa T, Chen SJ, Van Bommel D, Lin JS, Lin FF, Johansson SL, Christman JK, Lin MF. p66Shc protein is upregulated by steroid hormones in hormone-sensitive cancer cells and in primary prostate carcinomas. *Int. J. Cancer.* 2004; 108:672–678. [PubMed: 14696093]
- [21]. Veeramani S, Igawa T, Yuan TC, Lin FF, Lee MS, Lin JS, Johansson SL, Lin MF. Expression of p66(Shc) protein correlates with proliferation of human prostate cancer cells. *Oncogene.* 2005; 24:7203–7212. [PubMed: 16170380]
- [22]. Kumar S, Kumar S, Rajendran M, Alam SM, Lin FF, Cheng PW, Lin MF. Steroids up-regulate p66Shc longevity protein in growth regulation by inhibiting its ubiquitination. *PLoS One.* 2011; 6:e15942. [PubMed: 21264241]
- [23]. Rajendran M, Thomes P, Zhang L, Veeramani S, Lin MF. p66Shc-a longevity redox protein in human prostate cancer progression and metastasis: p66Shc in cancer progression and metastasis. *Cancer Metastasis Rev.* 2010; 29:207–222. [PubMed: 20111892]
- [24]. Raffo AJ, Perlman H, Chen MW, Day ML, Streitman JS, Buttyan R. Overexpression of bcl-2 protects prostate cancer cells from apoptosis in vitro and confers resistance to androgen depletion in vivo. *Cancer Res.* 1995; 55:4438–4445. [PubMed: 7671257]
- [25]. Oltvai ZN, Millman CL, Korsmeyer SJ. Bcl-2 heterodimerizes in vivo with a conserved homolog, Bax, that accelerates programmed cell death. *Cell.* 1993; 74:609–619. [PubMed: 8358790]
- [26]. Reid AH, Attard G, Ambrosine L, Fisher G, Kovacs G, Brewer D, Clark J, Flohr P, Edwards S, Berney DM, Foster CS, Fletcher A, Gerald WL, Møller H, Reuter VE, Scardino PT, Cuzick J, de Bono JS, Cooper CS. Transatlantic Prostate Group. Molecular characterisation of ERG, ETV1 and PTEN gene loci identifies patients at low and high risk of death from prostate cancer. *Br. J. Cancer.* 2010; 102:678–684. [PubMed: 20104229]
- [27]. Taylor BS, Schultz N, Hieronymus H, Gopalan A, Xiao Y, Carver BS, Arora VK, Kaushik P, Cerami E, Reva B, Antipin Y, Mitsiades N, Landers T, Dolgalev I, Major JE, Wilson M, Socci ND, Lash AE, Heguy A, Eastham JA, Scher HI, Reuter VE, Scardino PT, Sander C, Sawyers CL, Gerald WL. Integrative genomic profiling of human prostate cancer. *Cancer Cell.* 2010; 18:11–22. [PubMed: 20579941]
- [28]. Carver BS, Chapinski C, Wongvipat J, Hieronymus H, Chen Y, Chandarlapaty S, Arora VK, Le C, Koutcher J, Scher H, Scardino PT, Rosen N, Sawyers CL. Reciprocal feedback regulation of PI3K and androgen receptor signaling in PTEN-deficient prostate cancer. *Cancer Cell.* 2011; 19:575–586. [PubMed: 21575859]
- [29]. Feldman BJ, Feldman D. The development of androgen-independent prostate cancer. *Nat. Rev. Cancer.* 2001; 1:34–45. [PubMed: 11900250]
- [30]. Debes JD, Tindall DJ. Mechanisms of androgen refractory prostate cancer. *N. Engl. J. Med.* 2004; 351:1488–1490. [PubMed: 15470210]

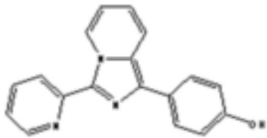
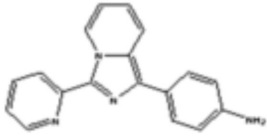
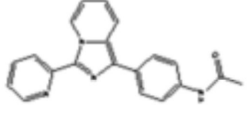
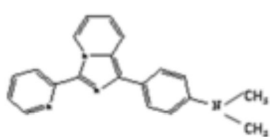
- [31]. Muniyan S, Ingersoll MA, Batra SK, Lin MF. Cellular prostatic acid phosphatase, a PTEN-functional homologue in prostate epithelia, functions as a prostate-specific tumor suppressor. *Biochim. Biophys. Acta*. 2014 (doi.org/10.1016/j.bbcan.2014.04.006).
- [32]. Pienta KJ, Bradley D. Mechanisms underlying the development of androgen-independent prostate cancer. *Clin. Cancer Res*. 2006; 12:1665–1671. [PubMed: 16551847]
- [33]. Fredericks WJ, Sepulveda J, Lai P, Tomaszewski JE, Lin MF, McGarvey T, Rauscher FJ 3rd, Malkowicz SB. The tumor suppressor TERE1 (UBIAD1) prenyltransferase regulates the elevated cholesterol phenotype in castration resistant prostate cancer by controlling a program of ligand dependent SXR target genes. *Oncotarget*. 2013; 4:1075–1092. [PubMed: 23919967]
- [34]. Miyashita T, Reed JC. Tumor suppressor p53 is a direct transcriptional activator of the human bax gene. *Cell*. 1995; 80:293–299. [PubMed: 7834749]
- [35]. O'Donnell A, Judson I, Dowsett M, Raynaud F, Dearnaley D, Mason M, Harland S, Robbins A, Halbert G, Nutley B, Jarman M. Hormonal impact of the 17 $\alpha$ -hydroxylase/C(17,20)-lyase inhibitor abiraterone acetate (CB7630) in patients with prostate cancer. *Br. J. Cancer*. 2004; 90:2317–2325. [PubMed: 15150570]
- [36]. Tran C, Ouk S, Clegg NJ, Chen Y, Watson PA, Arora V, Wongvipat J, Smith-Jones PM, Yoo D, Kwon A, Wasielewska T, Welsbie D, Chen CD, Higano CS, Beer TM, Hung DT, Scher HI, Jung ME, Sawyers CL. Development of a second-generation antiandrogen for treatment of advanced prostate cancer. *Science*. 2009; 324:787–790. [PubMed: 19359544]
- [37]. Ryan CJ, Smith MR, de Bono JS, Molina A, Logothetis CJ, de Souza P, Fizazi K, Mainwaring P, Piulats JM, Ng S, Carles J, Mulders PF, Basch E, Small EJ, Saad F, Schrijvers D, Van Poppel H, Mukherjee SD, Suttman H, Gerritsen WR, Flaig TW, George DJ, Yu EY, Efsthathiou E, Pantuck A, Winkquist E, Higano CS, Taplin ME, Park Y, Kheoh T, Griffin T, Scher HI, Rathkopf DE. COU-AA-302 Investigators. Abiraterone in metastatic prostate cancer without previous chemotherapy. *N. Engl. J. Med*. 2013; 368:138–148. [PubMed: 23228172]
- [38]. Sternberg CN, de Bono JS, Chi KN, Fizazi K, Mulders P, Cerbone L, Hirmand M, Forer D, Scher HI. Improved outcomes in elderly patients with metastatic castration-resistant prostate cancer treated with the androgen receptor inhibitor enzalutamide: results from the phase III AFFIRM trial. *Ann. Oncol*. 2014; 25:429–434. [PubMed: 24478320]
- [39]. Sun M, Yang L, Feldman RL, Sun XM, Bhalla KN, Jove R, Nicosia SV, Cheng JQ. Activation of phosphatidylinositol 3-kinase/Akt pathway by androgen through interaction of p85 $\alpha$ , androgen receptor, and Src. *J. Biol. Chem*. 2003; 278:42992–3000. [PubMed: 12933816]
- [40]. Veeramani S, Chou YW, Lin FC, Muniyan S, Lin FF, Kumar S, Xie Y, Lele SM, Tu Y, Lin MF. Reactive oxygen species induced by p66Shc longevity protein mediate nongenomic androgen action via tyrosine phosphorylation signaling to enhance tumorigenicity of prostate cancer cells. *Free Radic. Biol. Med*. 2012; 53:95–108. [PubMed: 22561705]
- [41]. Alam SM, Rajendran M, Ouyang S, Veeramani S, Zhang L, Lin MF. A novel role of Shc adaptor proteins in steroid hormone-regulated cancers. *Endocr. Relat. Cancer*. 2009; 16:1–16. [PubMed: 19001530]
- [42]. McDonnell TJ, Troncoso P, Brisbay SM, Logothetis C, Chung LW, Hsieh JT, Tu SM, Campbell ML. Expression of the proto-oncogene bcl-2 in the prostate and its association with emergence of androgen-independent prostate cancer. *Cancer Res*. 1992; 52:6940–6944. [PubMed: 1458483]
- [43]. Liu AY, Corey E, Bladou F, Lange PH, Vessella RL. Prostatic cell lineage markers: emergence of Bcl2+ cells of human prostate cancer xenograft LuCaP 23 following castration. *Int. J. Cancer*. 1996; 65:85–89. [PubMed: 8543402]
- [44]. Castilla C, Congregado B, Chinchón D, Torrubia FJ, Japón MA, Sáez C. Bcl-xL is overexpressed in hormone-resistant prostate cancer and promotes survival of LNCaP cells via interaction with proapoptotic Bak. *Endocrinology*. 2006; 147:4960–4967. [PubMed: 16794010]
- [45]. Martin SS, Ridgeway AG, Pinkas J, Lu Y, Reginato MJ, Koh EY, Michelman M, Daley GQ, Brugge JS, Leder P. Cytoskeleton-based functional genetic screen identifies Bcl-xL as an enhancer of metastasis, but not primary tumor growth. *Oncogene*. 2004; 23:4641–4645. [PubMed: 15064711]
- [46]. Zelivianski S, Spellman M, Kellerman M, Kakitelashvili V, Zhou XW, Lugo E, Lee MS, Taylor R, Davis TL, Hauke R, Lin MF. ERK inhibitor PD98059 enhances docetaxel-induced apoptosis

- of androgen-independent human prostate cancer cells. *Int. J. Cancer*. 2003; 107:478–485. [PubMed: 14506750]
- [47]. Miyashita T, Krajewski S, Krajewska M, Wang HG, Lin HK, Liebermann DA, Hoffman B, Reed JC. Tumor suppressor p53 is a regulator of bcl-2 and bax gene expression in vitro and in vivo. *Oncogene*. 1994; 9:1799–1805. [PubMed: 8183579]
- [48]. Hennessy BT, Smith DL, Ram PT, Lu Y, Mills GB. Exploiting the PI3K/AKT pathway for cancer drug discovery. *Nat. Rev. Drug Discov*. 2005; 4:988–1004. [PubMed: 16341064]
- [49]. Rhodes N, Heerding DA, Duckett DR, Eberwein DJ, Knick VB, Lansing TJ, McConnell RT, Gilmer TM, Zhang SY, Robell K, Kahana JA, Geske RS, Kleymenova EV, Choudhry AE, Lai Z, Leber JD, Minthorn EA, Strum SL, Wood ER, Huang PS, Copeland RA, Kumar R. Characterization of an Akt kinase inhibitor with potent pharmacodynamics and antitumor activity. *Cancer Res*. 2008; 68:2366–2374. [PubMed: 18381444]
- [50]. Kaarbø M, Mikkelsen OL, Malerød L, Qu S, Lobert VH, Akgul G, Halvorsen T, Maelandsmo GM, Saatcioglu F. PI3K-AKT-mTOR pathway is dominant over androgen receptor signaling in prostate cancer cells. *Cell. Oncol*. 2010; 32:11–27. [PubMed: 20203370]

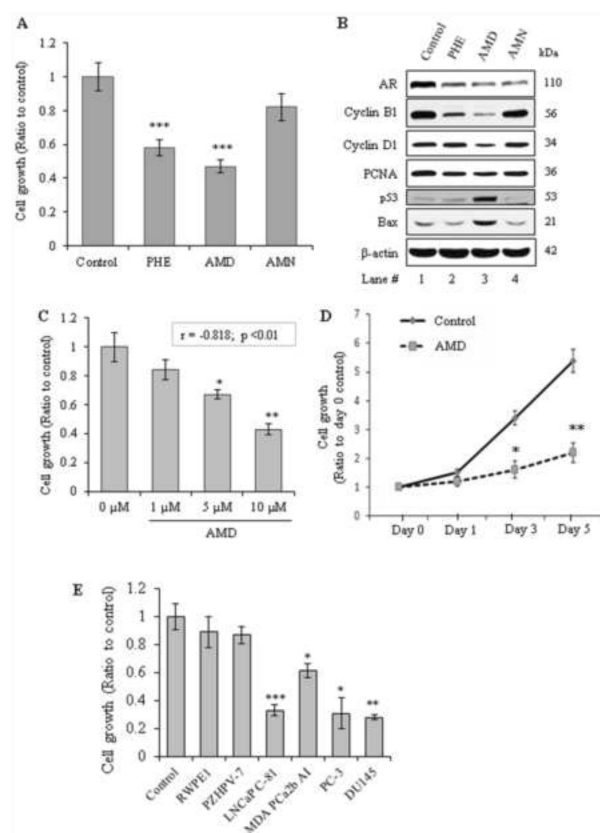


### Highlights

- The imidazopyridine family is a promising class of compounds to combat CR PCa.
- Members of this family can have differential effects on PCa vs. normal epithelia.
- These compounds decrease cancer cell proliferation and tumorigenicity.
- The inhibitory activity was in part due to the induction of apoptosis.
- Imidazopyridine compounds inhibit both AR and PI3K/Akt signaling pathways.

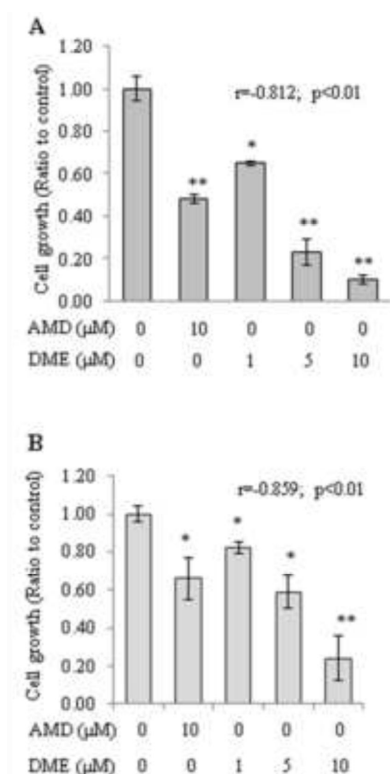
Name of the compound	Formula Weight	Structure
IMP-PHE	287.13	
IMP-AMD	286.33	
IMP-AMN	328.37	
IMP-DME	314.38	

**Fig. 1.**  
The structure of imidazopyridine derivatives.

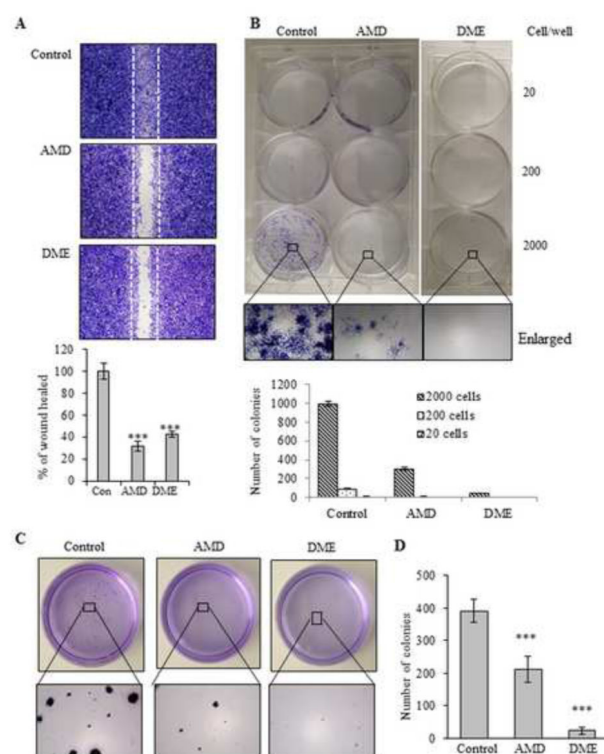
**Fig. 2.**

Effects of imidazopyridine derivatives on the growth of PCa cells in regular culture conditions. **A.** LNCaP C-81 cells were plated in six-well plates at  $2 \times 10^3$  cells/cm<sup>2</sup> in regular medium for three days, then 10  $\mu$ M each of imidazopyridine derivatives (PHE, AMN and AMD) in fresh medium were added for 72 hours. Cells were trypsinized and counted for live cell number. The results presented were mean  $\pm$  SD; n=2 $\times$ 3. \*\*\* $p$ <0.001. **B.** Total cell lysate proteins from imidazopyridine derivatives-treated C-81 cells were analyzed for AR, p53, Bax, cyclin B1, cyclin D1, PCNA proteins.  $\beta$ -actin protein level was analyzed and used as a loading control. **C.** The dose-dependent effect of AMD on LNCaP C-81 cell growth in regular culture medium. Cells were plated in six-well plates at  $2 \times 10^3$  cells/cm<sup>2</sup> in regular medium for three days and then treated with different concentrations of AMD in fresh medium. After 3 days, cells were trypsinized and counted for cell growth. The results presented were mean  $\pm$  SD; n=2 $\times$ 3. \* $p$ <0.05; \*\* $p$ <0.01. **D.** Time-dependent effect of AMD on LNCaP C-81 cell growth in regular culture condition. Cells were plated in six-well plates at  $2 \times 10^3$  cells/cm<sup>2</sup> in regular medium for three days, then 10  $\mu$ M AMD were added. One set of cells in triplicates was harvested after 1, 3 & 5 days, and counted for cell growth. The fresh medium was added to remaining cells on day 1 and 3. The results presented were mean  $\pm$  SE; n=2 $\times$ 3. \* $p$ <0.05; \*\* $p$ <0.01. **E.** Effects of AMD on the growth of various PCa cells and immortalized prostate epithelial cells. All cells were plated in six-well plates at the noted density in their respective medium for three days, then fresh media plus 10  $\mu$ M AMD were added. After 3 days cells were trypsinized and counted for cell number. The results presented were mean  $\pm$  SE; n=2 $\times$ 3. \* $p$ <0.05; \*\* $p$ <0.01; \*\*\* $p$ <0.001. RWPE1 -  $4 \times 10^3$

cells/cm<sup>2</sup>; PZ-HPV-7 -  $6 \times 10^3$  cells/cm<sup>2</sup>, LNCaP C-81 -  $2 \times 10^3$  cells/cm<sup>2</sup>; MDA PCa2b AI -  $3 \times 10^3$  cells/cm<sup>2</sup>; PC-3 -  $2 \times 10^3$  cells/cm<sup>2</sup>; DU145 -  $2 \times 10^3$  cells/cm<sup>2</sup>.

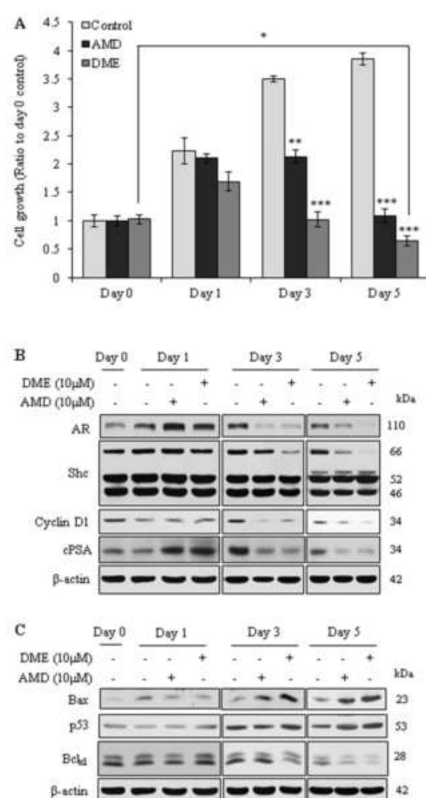
**Fig. 3.**

Effects of AMD and DME on LNCaP C-81 cell proliferation in regular and steroid-reduced culture conditions. **A.** The effects of AMD and DME on LNCaP C-81 cell growth in regular culture medium. Cells were plated in six-well plates at  $2 \times 10^3$  cells/cm<sup>2</sup> in regular medium for three days and then treated with 10  $\mu\text{M}$  of AMD and different doses of DME in fresh medium for 3 days. **B.** The effects of AMD and DME on LNCaP C-81 cells in steroid-reduced condition. Cells were plated in six-well plates at  $3 \times 10^3$  cells/cm<sup>2</sup> in regular medium for three days, followed by maintained in steroid-reduced media containing 1 nM DHT for two days. AMD and DME at different concentrations in fresh SR media containing 1 nM DHT were then added. After 3 days of treatment, cells were trypsinized and counted for cell numbers. The results presented were mean  $\pm$  SD;  $n=2 \times 3$ . \*  $p < 0.05$ ; \*\*  $p < 0.01$ .

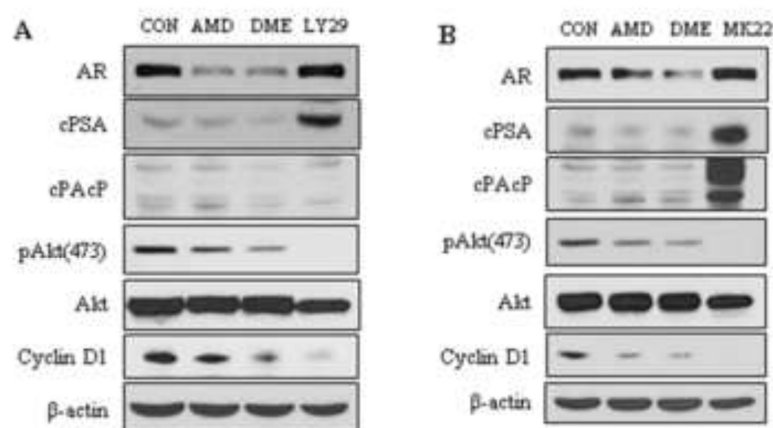
**Fig. 4.**

Effects of AMD and DME on PCa cell migration and tumorigenicity. **A.** PC-3 cells were seeded in a 6-well culture plate ( $1 \times 10^4$  cells/cm<sup>2</sup>) until 90% confluence. A wound was created on monolayer culture using 200  $\mu$ l pipette tip, and the cells were then treated with or without 10  $\mu$ M AMD or DME for 12 hours. At the end of the experiment, cells were stained, photographed and the migration inhibitory-potential of AMD and DME was determined by measuring the wound closure.  $n=2 \times 4$ , \*\*\* $p < 0.01$ . **B.** LNCaP C-81 cells were plated in plastic wares at the densities of 20, 200 and 2000 cells/well. After 24 hours the attached cells were treated with respective compounds at 10  $\mu$ M concentration of AMD and DME. The cells were fed on day 5 and 8 with fresh culture media with respective inhibitors. On day 10, the cells were stained and photographed. The bottom picture was the enlarged version under microscope and the colony number was counted. **C.** LNCaP C-81 cells were plated at the densities of  $5 \times 10^4$  cells/35mm dish in soft agar plates. At the end of 4 weeks, the colonies formed were stained and that from single cell was counted. Representative images of colony formation were shown. The lower panel is microscope enlarged images. **D.** Number of soft agar colonies in respective groups. The results presented were mean  $\pm$  SE;  $n=2 \times 4$ . \*\*\* $p < 0.01$ .



**Fig. 5.**

The kinetic effects of AMD & DME on LNCaP C-81 cells in steroid-reduced conditions. **A.** The cells were plated in six-well plates at  $2 \times 10^3$  cells/cm<sup>2</sup> in regular medium for three days, then steroid starved for 48 hours followed by treatment with AMD and DME at the concentration of 10  $\mu$ M. After 1, 3 & 5 days, one set of cells (in duplicates) from each group was harvested for cell number determination. The remaining cells were replenished with fresh medium and inhibitors (AMD & DME). **B.** Total cell lysate proteins from AMD- and DME-treated C-81 cells were analyzed for AR, Shc, PSA and cyclin D1 protein.  $\beta$ -actin protein level was used as a loading control. **C.** The pro-apoptotic effect of AMD & DME on LNCaP C-81 cells in a steroid-reduced condition with time dependent manner. Total cell lysate proteins from AMD and DME treatment were analyzed for p53, Bcl-X<sub>L</sub> and Bax proteins.  $\beta$ -actin protein level was used as a loading control. The results presented were mean  $\pm$  SE; n=2 $\times$ 3. \* $p$ <0.05; \*\* $p$ <0.01; \*\*\* $p$ <0.001.

**Fig. 6.**

Effects of AMD and DME on AR and PI3K/Akt signaling in LNCaP C-81 cells under steroid-reduced culture conditions. Cells were plated in T25 flasks at  $4 \times 10^3$  cells/cm<sup>2</sup> in regular medium for three days, then steroid starved for 48 hours followed by treatment with 10  $\mu$ M AMD, DME, PI3K inhibitor (LY294002) (A) or pan Akt inhibitor (MK2206) (B). Control cells (Con) received solvent alone. After 72 hours cells were harvested and analyzed for pAkt, AR, cPSA, cPAP (Cellular prostatic acid phosphatase, a PTEN-functional homologue in prostate epithelia, functions as a prostate-specific tumor suppressor) and cyclin D1 protein levels.  $\beta$ -actin protein level was used as a loading control.